

Non-Universal Spectra of Ultra-High Energy Cosmic Ray Primaries and Secondaries in a Structured Universe

Günter Sigl¹

¹*APC * (AstroParticules et Cosmologie), 10, rue Alice Domon et Léonie Duquet, 75205 Paris Cedex 13, France
and Institut d'Astrophysique de Paris, UMR 7095 CNRS - Université
Pierre & Marie Curie, 98 bis boulevard Arago, F-75014 Paris, France*

Analytical calculations of extra-galactic cosmic ray spectra above $\sim 10^{17}$ eV are often performed assuming continuous source distributions, giving rise to spectra that depend little on the propagation mode, be it rectilinear or diffusive. We perform trajectory simulations for proton primaries in the probably more realistic case of discrete sources with a density of $\sim 10^{-5}$ Mpc⁻³. We find two considerable non-universal effects that depend on source distributions and magnetic fields: First, the primary extra-galactic cosmic ray flux can become strongly suppressed below a few 10^{18} eV due to partial confinement in magnetic fields surrounding sources. Second, the secondary photon to primary cosmic ray flux ratio between $\simeq 3 \times 10^{18}$ eV and $\simeq 10^{20}$ eV decreases with decreasing source density and increasing magnetization. As a consequence, in acceleration scenarios for the origin of highest energy cosmic rays the fraction of secondary photons may be difficult to detect even for experiments such as Pierre Auger. The cosmogenic neutrino flux does not significantly depend on source density and magnetization.

PACS numbers: 98.70.Sa, 13.85.Tp, 98.65.Dx, 98.54.Cm

I. INTRODUCTION

A major unresolved aspect of ultra-high energy cosmic ray (UHECR) physics [1] is their composition and above which energy the flux is dominated by extragalactic sources. Above $\simeq 10^{17}$ eV the chemical composition is basically unknown [2]. Around 10^{18} eV the situation is particularly inconclusive as HiRes [3] and HiRes-MIA [4] data suggest a light (proton dominated) composition, whereas other experiments indicate a heavy composition [5].

As a consequence, there are currently two different scenarios: The "standard" one, where a transition from a steeper, galactic heavy component to a flatter, extragalactic component dominated by protons takes place at the ankle at $\simeq 5 \times 10^{18}$ eV, see, e.g., Ref. [6], and a more recent one suggesting that this transition actually takes place at lower energies, namely around the "second knee" at $\simeq 4 \times 10^{17}$ eV.

This second scenario in which extragalactic protons dominate down to the second knee has the following consequences: First, since the observed spectrum above the second knee is quite steep, $\propto E^{-3.3}$, the extragalactic proton flux has to cut off below $\simeq 4 \times 10^{17}$ eV. This can be explained as a magnetic horizon effect: Protons from cosmological distances cannot reach the observer any more within a Hubble time due to diffusion in large scale magnetic fields [7, 8, 9, 10, 11, 12]. Second, the ankle would have to be interpreted as due to pair production of the extragalactic protons [13, 14]. In particular, it has been pointed out recently [14, 15], that this model cannot af-

ford injection of a significant heavy component above the ankle whose secondary photo-disintegration products in the form of intermediate mass nuclei would produce a bump around the ankle. Injection of a mixed composition would also require a harder injection spectrum $\propto E^{-\alpha}$ with $\alpha \simeq 2.2$, as opposed to the extragalactic ankle scenario with pure protons [14] which requires an injection spectrum $\propto E^{-2.6}$.

In the proton dominated low-cross over scenario the resulting spectra are surprisingly insensitive to details such as extra-galactic magnetic fields (EGMF) and actual source distribution, as long as the distances between UHECR sources are much smaller than the energy loss and diffusion lengths [16, 17]. The spectra are then equal to the spectra resulting from a homogeneous source distribution which is therefore called "universal". Continuously distributed sources fulfill this condition.

Actual UHECR sources are, however, likely discrete with a relatively small density of order $\sim 10^{-5}$ Mpc⁻³ [18]. These values are motivated by the density of candidate sources such as active galaxies and also by hints of UHECR clusters. In addition, there likely is a strongly structured EGMF. In the present paper we study how a strongly structured Universe can cause deviations from the universal spectra in the case where extragalactic protons dominate the observed flux down to $\sim 10^{18}$ eV.

We also include in this study secondary neutrinos and γ -rays, produced by interactions of the primary nucleons with the cosmic microwave background (CMB) and the infrared (IR) background. The relevant reactions which also govern energy loss of the primary nucleons are pion production above the "GZK threshold" [19] and, for γ -rays, by pair production of protons. There is a strong motivation to study predictions for the fraction of γ -rays in the UHECR flux from recent experimental upper lim-

*UMR 7164 (CNRS, Université Paris 7, CEA, Observatoire de Paris)

its [20, 21, 22, 23, 24] that will further improve in the near future, especially from the Pierre Auger project [25]. Even secondary neutrino fluxes may be detectable in the not too far future [26].

In section 2 we describe our simulations, in section 3 we discuss results for various degrees of structure in the source distribution and magnetic field scenarios. In section 4 we discuss uncertainties in the γ -ray to charged primary flux ratio predicted in bottom-up scenarios and we conclude in section 4. We use natural units, $\hbar = c = k = 1$, throughout the paper.

II. NUMERICAL SIMULATIONS

For the trajectory simulations we use the public code package CRPropa [27, 28]. It follows nucleon trajectories in 3 dimensions in arbitrarily structured environments and takes into account secondary neutrinos and electromagnetic (EM) cascades produced by nucleon interactions with the CMB and IR backgrounds. Note that trajectory simulations allow to treat both the rectilinear and diffusive regime without approximation and are thus more general than using the diffusion approximation as adopted in Ref. [16, 17] which in addition was restricted to a homogeneous EGMF. We will also compare the general case to the isotropic situation in the absence of UHECR deflection and source structure which can be simulated with the one-dimensional version of CRPropa in which primary and secondary particles just propagate along straight lines. This case has been considered, e.g., in Ref. [29, 30].

We inject protons with a spectrum $E^{-\gamma}$ up to 10^{21} eV and adjust the injection index γ to the data. We also consider scenarios where the injection power per comoving volume evolves as a power law $\propto (1+z)^m$, where m is often called the “bright phase index”. We integrate up to redshift $z = 3$.

For nucleons we take into account photo-pion production, and pair production on the CMB and IR background, as well as redshift, and deflection in the cases where we consider an EGMF.

The γ -ray interaction length above $\sim 10^{19}$ eV strongly depends on the density of the universal radio background (URB) [31]. We use the minimal estimate for the URB [32]. For the IR background we use the model of Primack et al. [33]. The IR background is mostly relevant for pion production for relatively steep proton injection spectra, and for photon attenuation in the TeV regime. Since we are mostly interested in energies above $\sim 10^{17}$ eV, for our purposes the IR background is less relevant for EM cascade propagation. Between $\sim 10^{17}$ eV and $\sim 10^{21}$ eV, the γ -ray attenuation length is smaller than 10 Mpc, and thus redshift effects are negligible at these energies. Furthermore, since we are interested in diffuse fluxes, we can treat the EM cascades as 1-dimensional.

Neutrinos propagate along straight lines and, once pro-

duced, are only subject to redshift.

The concordance cosmology is used for which, assuming a flat Universe, the Hubble rate $H(z)$ at redshift z in the matter dominated regime, $z \lesssim 10^3$, is given by $H(z) = H_0 [\Omega_m(1+z)^3 + \Omega_\Lambda]^{1/2}$. We use the standard values being $\Omega_m = 0.3$, $\Omega_\Lambda = 0.7$, and $H_0 = h_0 100 \text{ km s}^{-1} \text{ Mpc}^{-1}$ with $h_0 = 0.72$.

III. RESULTS

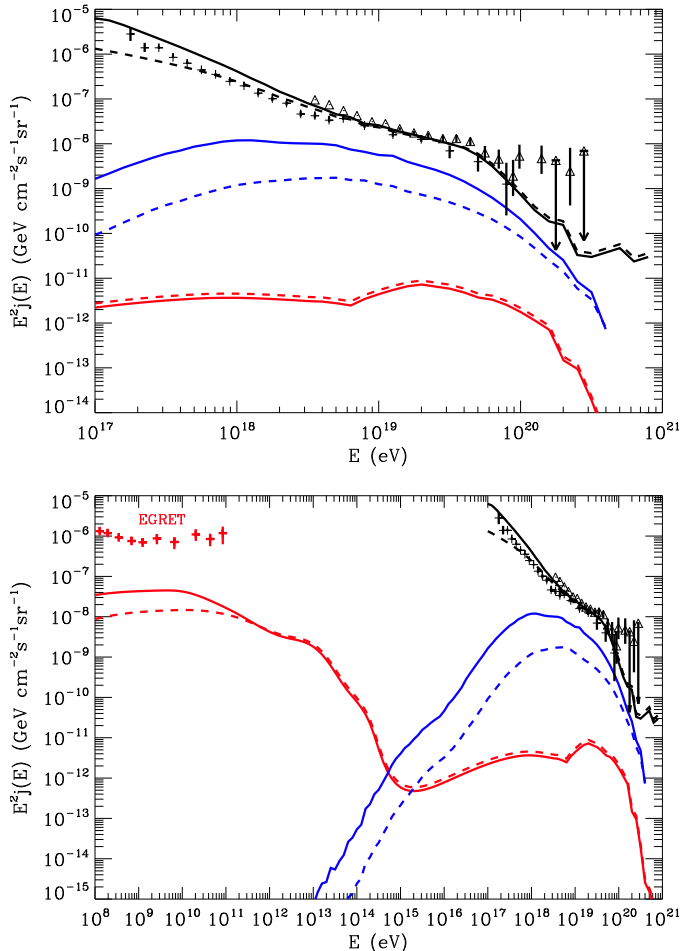


FIG. 1: Upper panel: Fluxes of primary nucleons (black), secondary photons (red) and neutrinos per flavor (blue) for a homogeneous source distribution injecting an $E^{-2.6}$ proton spectrum up to 10^{21} eV and up to redshift $z = 3$. The dashed lines are in absence of redshift evolution, the solid lines are for a bright phase index $m = 3$. No magnetic fields are taken into account and fluxes have been computed with the one dimensional version of CRPropa. AGASA data [34] are shown as triangles, HiRes data [35] as crosses. Lower panel: Same over a wider energy range. Also shown is the diffuse γ -ray flux that has been observed by EGRET [36].

In Fig. 1 we show nucleon, γ -ray and neutrino fluxes for a Universe filled with homogeneously distributed

sources, with and without source evolution. As pointed out in Ref. [13, 17], the HiRes and AGASA spectra can be made to give a consistent ankle structure, coincident with the theoretically predicted ankle position at $\simeq 5 \times 10^{18}$ eV, by multiplying the HiRes energies with a factor 1.2 and the AGASA energies with a factor 0.9. This is best seen by multiplying the differential spectrum with E^3 , as shown in Fig. 2. The best fit to the observed flux down to $\simeq 2 \times 10^{17}$ eV then gives an injection spectral index of $2.6 \lesssim \gamma \lesssim 2.7$, where the lower value corresponds to $m \simeq 3$ and the upper value to $m \simeq 0$.

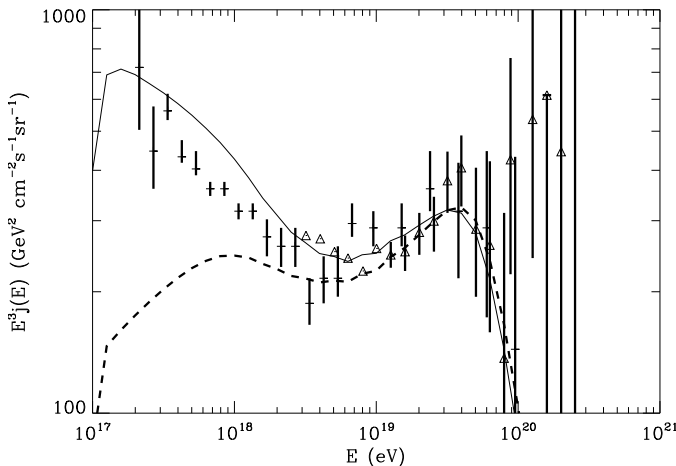


FIG. 2: Same as Fig. 1, upper panel, but with the energies measured by HiRes and AGASA multiplied by a factor of 1.2 and 0.9, respectively, and showing the differential nucleon flux multiplied by E^3 .

As the lower panel of Fig. 1 of shows, the γ -ray flux at GeV energies can reach about ten percent of the diffuse background observed by EGRET [36] in this scenario, particularly for significant source evolution. The energy in GeV γ -rays is comparable to the energy in primary cosmic rays at $\simeq 2 \times 10^{18}$ eV, where the proton energy attenuation length due to pair production becomes comparable to the Hubble radius [31]. A diffuse γ -ray flux at this level should be testable in the near future [37].

As in our earlier work in Refs. [38], for the scenarios with structured source distributions and/or magnetic fields we will in the following use the unconstrained large scale structure (LSS) simulations based on Refs. [39, 40]. A cross-section through the baryon density and magnetic field strength of the LSS simulation box is shown in Fig. 3. The EGMF in these simulations have been evolved passively and normalized to $\sim \mu$ Gauss in the centers of galaxy clusters. These EGMF are highly structured in that they reach a few microGauss in the most prominent structures such as galaxy clusters, but is $\lesssim 10^{-11}$ G in the voids. We note that the EGMF in this LSS simulation are relatively extended compared to other simulations [41] and current observations do not allow to distinguish between such different EGMF scenarios. The EGMF obtained in Ref. [41] is closer to the

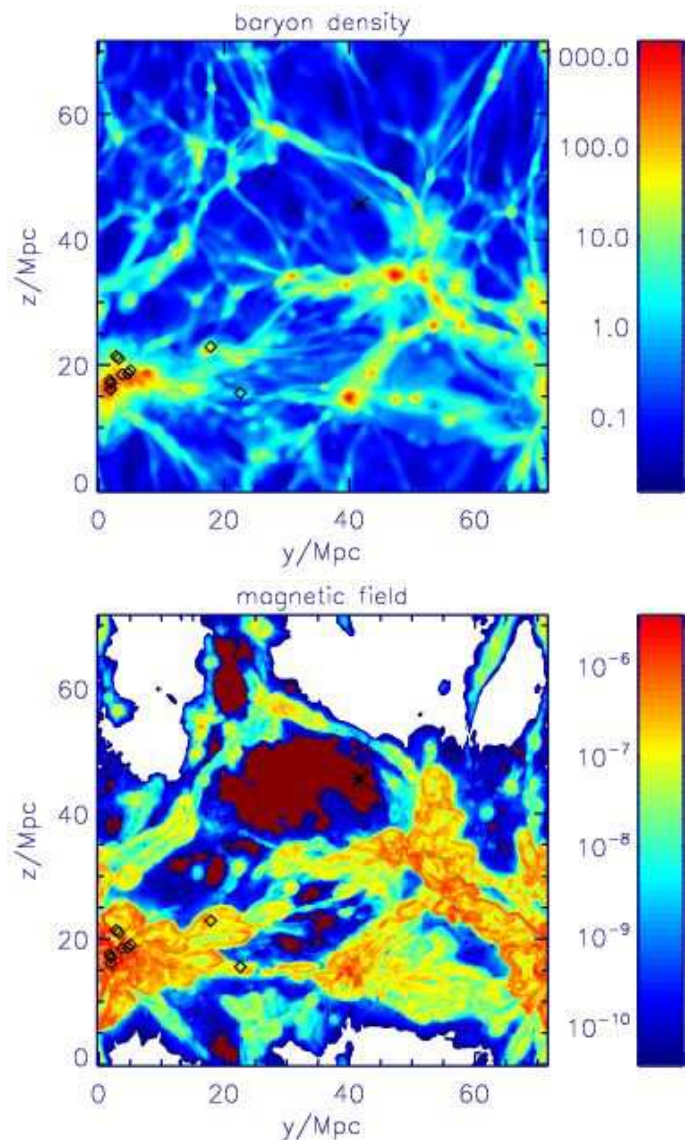


FIG. 3: Cross-section through the LSS simulation box from Refs. [39, 40] used in this study. The observer position is marked as a black cross near the center. The approximate positions of the ten sources in the discrete source realization investigated below are shown as black diamonds. Note that the simulation box including EGMF and sources is periodically repeated in all three directions. Upper panel: Baryon density. Lower panel: magnetic field strength for the EGMF considered. The field polarizations are not shown and are in general a combination of smooth and stochastic components.

case of negligible EGMF that we also study here.

Since the LSS simulation covers a volume of only $\simeq (75 \text{ Mpc})^3$, the structures and fields in the simulation box are periodically repeated in all three directions. In this way, no evolution of the structure and fields with redshift is taken into account. This is sufficient within the uncertainties in such scenarios since at distances larger than the GZK distance, spectra and angular distributions are insensitive to the detailed structure. The observer is

chosen in a low magnetic field region of the simulation box, resembling Earth's actual environment, as can be seen in Fig. 3.

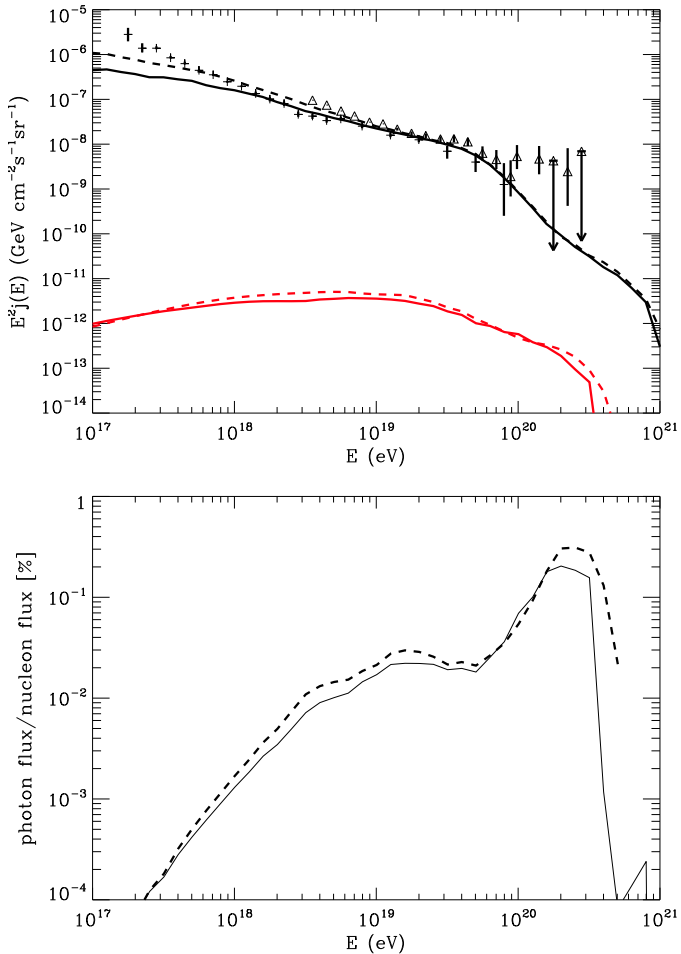


FIG. 4: Upper panel: Fluxes of primary nucleons (black) and secondary photons (red) for continuous sources following the baryon density of the LSS simulation in Refs. [39, 40] and injecting an $E^{-2.6}$ proton spectrum up to 10^{21} eV and redshift $z = 3$ with no source evolution, $m = 0$. Solid line assume the EGMF from these LSS simulations, whereas dashed lines are for negligible EGMF. Data as in Fig. 1. Lower panel: Photon to cosmic ray flux ratio for this case.

Fig. 4 shows results for structured, but continuous sources whose density is assumed proportional to the baryon density in the LSS simulation of which a cross-section is shown in Fig. 3. This time, the case with negligible EGMF is compared with the EGMF obtained from the LSS simulations, as in Refs. [38]. The spectra are hardly different from the homogeneous case shown in Fig. 1. This scenario therefore corresponds to the universal spectrum discussed in Ref. [16]. The proton flux is only slightly suppressed by the EGMF at a few 10^{18} eV. The neutral fraction, shown in the lower panel of Fig. 4 is also quite insensitive to both the continuous source distribution and the EGMF. It is at the lower end of the

range obtained in Ref. [29, 30].

In the following we define the photon to cosmic ray flux ratio as relative to the total observed cosmic ray flux below 3×10^{19} eV and relative to the simulated nucleon flux above 3×10^{19} eV. This photon to cosmic ray flux ratio, also shown in Fig. 4, in fact broadly follows the attenuation length of the EM cascade [31]. This is to be expected as long as the primary flux does not exhibit a strong break between the energy E at which the secondary to primary ratio is considered and the energies $E' > E$ of the primaries mostly responsible for the secondary flux at energy E . Below we will see that below $\simeq 3 \times 10^{18}$ eV and above $\simeq 10^{20}$ eV, the photon to nucleon ratio indeed depends little on source distributions and magnetization and mostly follows the behavior of the EM cascade attenuation length. Since in the combined CMB and URB this length scale increases roughly linearly with energy between $\simeq 10^{20}$ eV and $\simeq 10^{21}$ eV [31], this leads to a rise in the photon to nucleon ratio up to the order of 1 percent in this energy range. Unfortunately, due to the sharp drop of the primary cosmic ray flux expected at these energies, a photon to nucleon ratio of order percent may not be easier to detect than an order 10^{-4} ratio at lower energies.

We now consider a specific realization with discrete sources of density $n_s \sim 3 \times 10^{-5} \text{ Mpc}^{-3}$. As Fig. 3 shows, the sources in this realization are concentrated around the most prominent galaxy cluster. The spectra resulting in this scenario are shown in Fig. 5, upper panel. Both above the GZK energy around 10^{20} eV and below $\simeq 3 \times 10^{18}$ EeV the primary spectra are not universal any longer. This is understandable because the average source distance ~ 30 Mpc is now comparable to the GZK distance. Further, a cosmic ray of energy E in a region permeated by magnetic fields B has a Larmor radius $r_L \sim 1 (E/\text{EeV})(B/\mu\text{G})^{-1}$ kpc and during the lifetime of the Universe, $t_u \sim 10$ Gyr, diffuses a distance

$$l_d(E) \sim (r_L t_u)^{1/2} \sim 2 \left(\frac{E}{\text{EeV}} \right)^{1/2} \left(\frac{B}{\mu\text{G}} \right)^{-1/2} \text{ Mpc}, \quad (1)$$

as long as this length scale is smaller than the spatial extent of the field. Fig. 3 shows that the structured EGMF reaches values of $B \sim 0.1 \mu\text{G}$ over several Mpc around the sources in the LSS simulation used here. Below $\sim 3 \times 10^{18}$ eV, the diffusion length then also becomes smaller than the average source distance

$$d_s \simeq n_s^{-1/3} \simeq 46 \left(\frac{n_s}{\text{Mpc}^{-3}} \right)^{-1/3} \text{ Mpc}. \quad (2)$$

This leads to a suppression of the nucleon flux due to a partial confinement of UHECRs which was discussed qualitatively in Ref. [11]. Note that this is not quite the same as the magnetic horizon effect discussed in Refs [7, 11, 12, 42] where typically uniform EGMFs were assumed which is less realistic in a structured universe.

Above the threshold for pair production by photons with the CMB at $\simeq 10^{15}$ eV and up to $\simeq 10^{20}$ eV, the

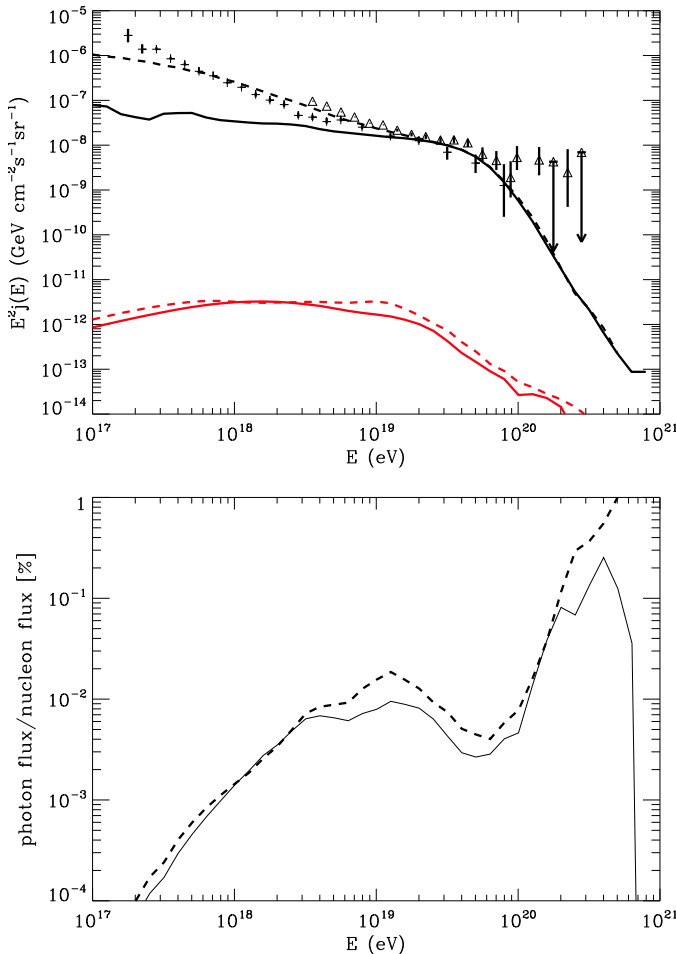


FIG. 5: Same as Fig. 4 for the discrete source realization with 10 sources in the LSS simulation box, see Fig. 3, injecting an $E^{-2.6}$ proton spectrum up to 10^{21} eV and redshift $z = 3$ with no source evolution, $m = 0$. This corresponds to a source density of $\simeq 3 \times 10^{-5} \text{ Mpc}^{-3}$. Again, solid line assume the EGMF from the LSS simulations, whereas dashed lines are for negligible EGMF, and no source evolution is assumed.

photon attenuation length is smaller than 10 Mpc [31]. Photons in this energy range thus have to be produced within $\lesssim 10$ Mpc from the observer. Above $\simeq 3 \times 10^{18}$ eV γ -rays are mostly produced by nucleons above the GZK threshold whose attenuation length is smaller than the typical source distance Eq. (2). This explains why the photon fraction of the UHECR flux between $\simeq 3 \times 10^{18}$ eV and $\simeq 10^{20}$ eV decreases with decreasing discrete source density. Furthermore, magnetic fields $\gtrsim 10^{-10}$ G effectively block cascade development and more EM energy is channeled into synchrotron radiation, ending up at GeV-TeV energies. This explains why the photon to charged cosmic ray ratio also decreases somewhat with increasing EGMF. Both tendencies are seen by comparing Figs. 4 and 5, lower panels.

In contrast, below $\simeq 3 \times 10^{18}$ eV, a good fraction of the photons are produced by pair production of protons at

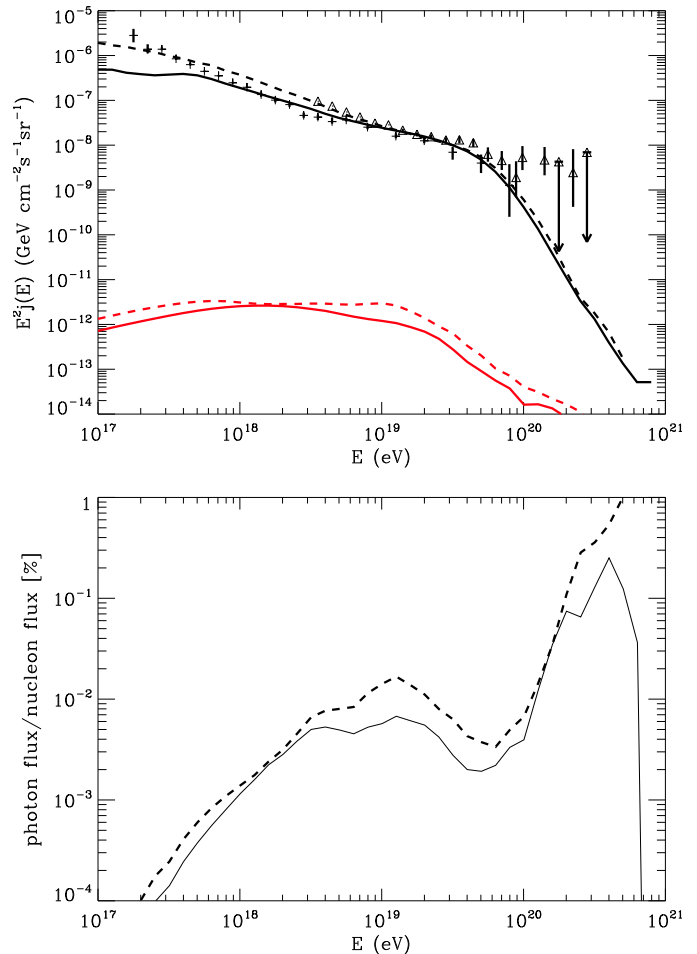


FIG. 6: Same as Fig. 5 for the discrete source realization, but now the spectra resulting for negligible EGMF (dashed lines) and with the EGMF (solid lines) are compared for different injection parameters, namely $m = 0$, $E^{-2.7}$ for the case without EGMF and $m = 3$, $E^{-2.7}$ for the case with EGMF.

energies below the GZK threshold. These protons have attenuation lengths larger than the typical source distance Eq. (2). Furthermore, at these energies the EM attenuation length decreases to below a few Mpc and the cascade flux thus depends mostly on the environment of the observer within a few Mpc where the EGMF is negligible, see Fig. 3. These two facts explain why below $\simeq 3 \times 10^{18}$ eV the photon to cosmic ray flux ratio is relatively insensitive to discrete source densities and magnetic environments, as confirmed by Figs. 4 and 5, lower panels. In contrast, this ratio does decrease with increasing magnetic fields around the observer if these fields are $\gtrsim 10^{-10}$ G, as we will see below for an EGMF with homogeneous statistical properties.

In Figs. 6 and 7 we compare the spectra in the scenarios with and without EGMF for different source evolutions, namely $m = 3$ and $m = 0$, respectively, for an injection spectrum $\propto E^{-2.7}$. In the case with EGMF, even for strong redshift evolution, a new low-energy, presum-

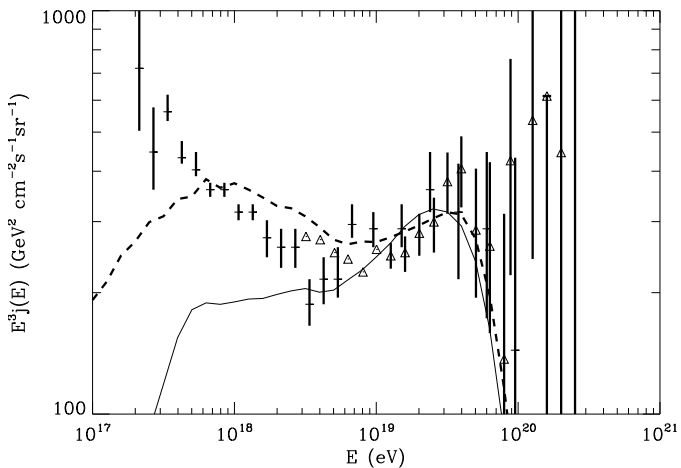


FIG. 7: Same as Fig. 6, upper panel, but with the energies measured by HiRes and AGASA multiplied by a factor of 1.2 and 0.9, respectively, and showing the differential nucleon flux multiplied by E^3 .

ably galactic component becomes necessary below a few 10^{18} eV. Furthermore, in this case the neutral fractions shown in the lower panel of Fig. 6 extend considerably below the lower limit obtained in Ref. [29, 30] which did not consider structured sources and EGMF.

Finally, in order to elucidate the role of the structure of the EGMF, we consider an EGMF with homogeneous properties: Its Fourier transform follows a power law spectrum, $|\mathbf{B}(k)|^2 \propto k^{-2.5}$ for $(75 \text{ Mpc})^{-1} \lesssim k \lesssim (0.6 \text{ Mpc})^{-1}$, with an r.m.s. strength of 10^{-9} G. This mimicks the scenarios considered in Ref. [11] of an EGMF with a coherence length $\simeq 1$ Mpc. The field strength is at the high end of realistic values, but still consistent with current upper limits [43]. Fig. 8 compares the resulting spectra with the case of negligible EGMF. Comparing the upper panels of Figs. 5 and Fig. 8, we see that even in this relatively strong EGMF with homogeneous properties, the proton flux suppression due to the magnetic horizon effect is considerably more modest than the confinement effect for the structured EGMF envisaged here.

In the lower panel of Fig. 8 we see that an EGMF of strength $\gtrsim 10^{-10}$ G with homogeneous properties tends to suppress the photon to cosmic ray flux ratio also at energies below $\simeq 3 \times 10^{18}$ eV, as was found already in Ref. [44] and also seen in Ref. [29, 30]. As remarked above, this is to be expected because the EM cascade development at these energies mostly depends on the magnetization of the environment of the observer within a few Mpc.

Note that the injection spectra needed in the scenarios discussed here where the cross over to extra-galactic cosmic rays occurs at a few 10^{17} eV is much steeper than predicted by most acceleration scenarios, but could be explained as an effective spectrum obtained by averaging over sources with different maximal energies and harder individual spectra [45].

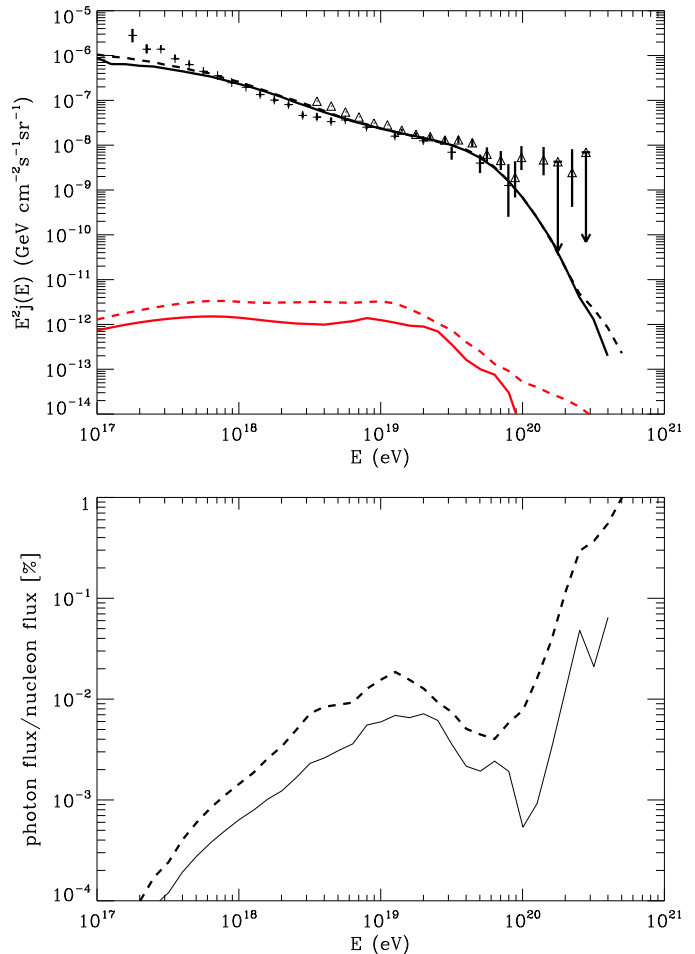


FIG. 8: As in Figs. 5 and 6 for the discrete source realization injecting an $E^{-2.6}$ proton spectrum in the absence of redshift evolution, $m = 0$, but now the spectra resulting for negligible EGMF (dashed lines) are compared with the spectra for a stochastic EGMF of strength 10^{-9} G and effective coherence length $\simeq 1$ Mpc (solid line), see text for details.

The proton injection power required for the scenarios shown in Figs. 5-7 is $\sim 7 \times 10^{37} \text{ erg s}^{-1} \text{ Mpc}^{-3}$ for negligible EGMF and about a factor 10 higher, $\sim 6 \times 10^{38} \text{ erg s}^{-1} \text{ Mpc}^{-3}$, in the presence of the EGMF considered here. The number for negligible fields is consistent with the power obtained in Ref. [42] which only considered relatively weak, unstructured EGMF. The orders of magnitude are consistent with acceleration in active galactic nuclei, for example.

All the scenarios discussed here are consistent with present data in terms of large scale isotropy and auto-correlations. However, an increase of the current world exposure by a factor of a few predicts significant large scale anisotropy as well as small-scale clustering, at least in the case of modest EGMF. Absence of such effects would hint to a relatively strong EGMF, as demonstrated in Fig. 9, or to a considerably higher source density.

We also found that the diffuse cosmogenic neutrino

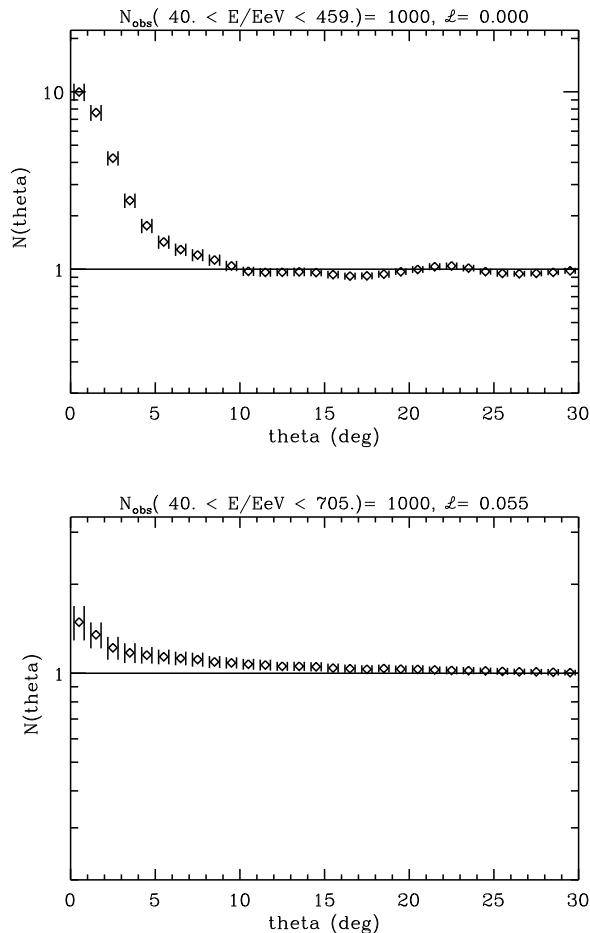


FIG. 9: Autocorrelation function of UHECR in the discrete source scenarios shown in Figs. 5 and 6, assuming 10^3 events observed above 40 EeV, a factor 5 – 10 above the current world data set. An angular resolution of 1° was assumed. Upper panel: No EGMF. Lower panel: Assuming the EGMF from the LSS simulation.

flux depends mostly on the source evolution, but little on the source distribution or EGMF. This is understandable because the neutrino energy attenuation length is basically the Hubble radius and thus always larger than all other scales involved. Sources up to cosmological distances thus contribute to the diffuse neutrino flux. Since neutrinos are produced by pionproduction of nucleons off the CMB and IR backgrounds, for a given UHECR injection spectrum, the fraction of the UHECR energy transformed to neutrinos should, therefore, be rather independent of source distribution or EGMF. Our neutrino fluxes are comparable to other calculations in the literature, for example Ref. [46]. A possible enhancement of cosmogenic neutrino fluxes from the source environment could come from an enhancement of the IR background around sources such as galaxy clusters, an effect we have not taken into account in the present work. One case in which this possibility was considered [47] does, however,

not give much higher diffuse neutrino fluxes when the constraint from the primary UHECR flux is taken into account.

IV. UNCERTAINTIES IN THE PHOTON TO CHARGED COSMIC RAY FLUX RATIO

If the actual but poorly known URB is larger than the minimal URB we used in the simulations presented in the previous section, photon absorption will be stronger, further reducing the photon to cosmic ray fraction.

A significant fraction of heavier nuclei of atomic number A in the primary UHECR flux is likely to reduce the photon to charged cosmic ray flux ratio above $\sim 10^{19}$ eV: Pion-production is shifted down by a factor $\simeq A$ in energy, falling below $\sim 10^{19}$ eV already for moderate A . An additional source of γ -rays is from photo-spallation of nuclei [48]. But these photons have an energy of $\sim \Gamma_A \times$ a few MeV which for Lorentz factors $\Gamma_A \lesssim 10^{11}$ is below $\sim 10^{18}$ eV. We recall in this context that the cosmogenic neutrino flux is also believed to considerably depend on primary cosmic ray composition [49, 50, 51].

On the other hand, additional photons could be produced in nucleon interactions with an IR background that could be enhanced around sources such as galaxy clusters, or by nucleon interactions with the ambient baryon gas in the sources. Both these possibilities have not been taken into account in the present work. However, we do not expect that these effects could significantly increase the photon fraction above $\sim 10^{15}$ eV for the following reasons: First, as discussed in Sect. III above, since in this energy range, the EM cascade attenuation length is smaller than or comparable to the typical source distance, the photon fraction depends mostly on EM secondary production outside the sources. Second, the primary cosmic ray flux is not expected to be significantly modified by these processes, since only about 1% of its energy is expected to be converted by interactions with an enhanced IR background within galaxy clusters [47], and since the optical depth for pp interactions is less than unity in galaxy clusters [52].

V. CONCLUSIONS

We have performed simulations following ultra-high energy nucleon trajectories above 10^{17} eV and compared scenarios with continuous and discrete source distributions as well as the case of negligible and highly structured extragalactic magnetic fields reaching microGauss levels in galaxy clusters. Powerful ultra-high energy cosmic ray sources likely have densities of order 10^{-5} Mpc^{-3} . We find two considerably non-universal effects that depend on source distributions and magnetic fields: We found that the primary extra-galactic cosmic ray flux can become strongly suppressed below a few 10^{18} eV if the sources are immersed in highly structured magnetic

fields. This is due to the fact that cosmic ray primaries start to be magnetically confined and do not reach the observer any more at these energies. This effect can indeed be considerably stronger than for stochastic magnetic fields with homogeneous properties and r.m.s. strength $\lesssim 10^{-9}$ G. We also found that the secondary photon to primary cosmic ray flux ratio between $\simeq 3 \times 10^{18}$ eV and $\simeq 10^{20}$ eV is of the order 10^{-4} and decreases with decreasing source density and increasing magnetization. In principle at least, this ratio could therefore serve as an independent measure of these poorly known quantities. In contrast, the photon to cosmic ray flux ratio is rather insensitive to source distributions and magnetic fields at lower energies as well as above $\simeq 10^{20}$ eV where it can reach the percent level. We also pointed out that a significant contribution of nuclei heavier than hydrogen to the primary cosmic ray flux tends to reduce the γ -ray to charged cosmic ray ratio further. Also, additional photon production within the sources is unlikely to increase

this ratio significantly. As a consequence, in acceleration scenarios for the origin of highest energy cosmic rays the fraction of secondary photons may be difficult to detect even for experiments such as Pierre Auger. In contrast, the cosmogenic neutrino flux does not significantly depend on source density and magnetization, but mostly on the redshift evolution of the sources.

Acknowledgments

This work partly builds on earlier collaborations with Eric Armengaud and Francesco Miniati. We thank Eric Armengaud and Markus Risse for stimulating exchanges and useful comments. During finishing this manuscript, we became aware of a draft by Gelmini, Kalashev and Semikoz [30] which studies the γ -ray to cosmic ray ratio in a one-dimensional setting.

-
- [1] for a recent review see, e.g., J. W. Cronin, “The highest-energy cosmic rays,” Nucl. Phys. Proc. Suppl. **138**, 465 (2005) [arXiv:astro-ph/0402487].
- [2] A. A. Watson, “The mass composition of cosmic rays above 10^{17} -eV,” Nucl. Phys. Proc. Suppl. **136**, 290 (2004) [arXiv:astro-ph/0408110].
- [3] R. U. Abbasi *et al.* [The High Resolution Fly’s Eye Collaboration], “A study of the composition of ultra high energy cosmic rays using the High Resolution Fly’s Eye,” Astrophys. J. **622**, 910 (2005) [arXiv:astro-ph/0407622].
- [4] T. Abu-Zayyad *et al.* [HiRes-MIA Collaboration], “Measurement of the cosmic ray energy spectrum and composition from 10^{17} -eV to $10^{18.3}$ -eV using a hybrid fluorescence technique,” Astrophys. J. **557**, 686 (2001) [arXiv:astro-ph/0010652].
- [5] J. R. Hoerandel, “Models of the knee in the energy spectrum of cosmic rays,” Astropart. Phys. **21**, 241 (2004) [arXiv:astro-ph/0402356].
- [6] T. Wibig and A. W. Wolfendale, “At what particle energy do extragalactic cosmic rays start to predominate?,” J. Phys. G **31**, 255 (2005) [arXiv:astro-ph/0410624].
- [7] C. Isola, M. Lemoine and G. Sigl, “Centaurus A as the source of ultra-high energy cosmic rays?,” Phys. Rev. D **65**, 023004 (2002) [arXiv:astro-ph/0104289].
- [8] T. Stanev, D. Seckel and R. Engel, “Propagation of ultra-high energy protons in regular extragalactic magnetic fields,” Phys. Rev. D **68**, 103004 (2003) [arXiv:astro-ph/0108338].
- [9] T. Stanev, “On the luminosity of the ultra high energy cosmic rays sources,” arXiv:astro-ph/0303123.
- [10] O. Deligny, A. Letessier-Selvon and E. Parizot, “Magnetic Horizons Of Uhecr Sources And The Gzk Feature,” Astropart. Phys. **21**, 609 (2004) [arXiv:astro-ph/0303624].
- [11] M. Lemoine, “Extra-galactic magnetic fields and the second knee in the cosmic-ray spectrum,” Phys. Rev. D **71**, 083007 (2005) [arXiv:astro-ph/0411173].
- [12] R. Aloisio and V. S. Berezhinsky, “Anti-GZK effect in UHECR diffusive propagation,” Astrophys. J. **625**, 249 (2005) [arXiv:astro-ph/0412578].
- [13] V. Berezhinsky, A. Z. Gazizov and S. I. Grigorieva, “On astrophysical solution to ultra high energy cosmic rays,” Phys. Rev. D **74**, 043005 (2006) [arXiv:hep-ph/0204357].
- [14] V. Berezhinsky, A. Z. Gazizov and S. I. Grigorieva, “Dip in UHECR spectrum as signature of proton interaction with CMB,” Phys. Lett. B **612**, 147 (2005) [arXiv:astro-ph/0502550].
- [15] D. Allard, E. Parizot, E. Khan, S. Goriely and A. V. Olinto, “UHE nuclei propagation and the interpretation of the ankle in the cosmic-ray spectrum,” arXiv:astro-ph/0505566.
- [16] R. Aloisio and V. Berezhinsky, “Diffusive propagation of UHECR and the propagation theorem,” Astrophys. J. **612**, 900 (2004) [arXiv:astro-ph/0403095].
- [17] R. Aloisio, V. Berezhinsky, P. Blasi, A. Gazizov, S. Grigorieva and B. Hnatyk, “A dip in the UHECR spectrum and the transition from galactic to extragalactic cosmic rays,” arXiv:astro-ph/0608219; and refs therein.
- [18] M. Kachelriess and D. Semikoz, “Ultra-high energy cosmic rays from a finite number of point sources,” Astropart. Phys. **23**, 486 (2005) [arXiv:astro-ph/0405258].
- [19] K. Greisen, “End To The Cosmic Ray Spectrum?,” Phys. Rev. Lett. **16**, 748 (1966); G. T. Zatsepin and V. A. Kuzmin, “Upper Limit Of The Spectrum Of Cosmic Rays,” JETP Lett. **4**, 78 (1966) [Pisma Zh. Eksp. Teor. Fiz. **4**, 114 (1966)].
- [20] K. Shinozaki *et al.*, “Upper limit on gamma-ray flux above 10^{19} -eV estimated by the Akeno Giant Air Shower Array experiment,” Astrophys. J. **571**, L117 (2002).
- [21] M. Risse *et al.*, “Upper limit on the photon fraction in highest-energy cosmic rays from AGASA data,” Phys. Rev. Lett. **95**, 171102 (2005) [arXiv:astro-ph/0502418].
- [22] G. I. Rubtsov *et al.*, “Upper limit on the ultra-high-energy photon flux from AGASA and Yakutsk data,” Phys. Rev. D **73**, 063009 (2006) [arXiv:astro-ph/0601449].
- [23] J. Abraham *et al.* [Pierre Auger Collaboration], “An up-

- per limit to the photon fraction in cosmic rays above 10^{19} eV from the Pierre Auger observatory,” *Astropart. Phys.* **27**, 155 (2007) [arXiv:astro-ph/0606619].
- [24] A. V. Glushkov, D. S. Gorbunov, I. T. Makarov, M. I. Pravdin, G. I. Rubtsov, I. E. Sleptsov and S. V. Troitsky, “Constraining the fraction of primary gamma rays at ultra-high energies from the muon data of the Yakutsk extensive-air-shower array,” arXiv:astro-ph/0701245.
- [25] M. Risse and P. Homola, “Search for ultra-high energy photons using air showers,” *Mod. Phys. Lett. A* (2007), in press; [arXiv:astro-ph/0702632].
- [26] A. B. McDonald, C. Spiering, S. Schonert, E. T. Kearns and T. Kajita, “Astrophysical neutrino telescopes,” *Rev. Sci. Instrum.* **75**, 293 (2004) [arXiv:astro-ph/0311343].
- [27] see <http://apcauger.in2p3.fr//CRPropa>.
- [28] E. Armengaud, G. Sigl, T. Beau and F. Miniati, “CRPropa: A numerical tool for the propagation of UHE cosmic rays, gamma-rays and neutrinos,” arXiv:astro-ph/0603675.
- [29] G. Gelmini, O. Kalashev and D. V. Semikoz, “GZK photons as ultra high energy cosmic rays,” arXiv:astro-ph/0506128.
- [30] G. Gelmini, O. Kalashev and D. V. Semikoz, “GZK photons in the minimal ultra high energy cosmic rays model,” arXiv:astro-ph/0702464.
- [31] see, e.g., P. Bhattacharjee and G. Sigl, “Origin and propagation of extremely high energy cosmic rays,” *Phys. Rept.* **327**, 109 (2000) [arXiv:astro-ph/9811011].
- [32] R. J. Protheroe and P. L. Biermann, “A new estimate of the extragalactic radio background and implications for ultra-high-energy gamma ray propagation,” *Astropart. Phys.* **6**, 45 (1996) [Erratum-ibid. **7**, 181 (1997)] astro-ph/9605119.
- [33] see, e.g., J. R. Primack, J. S. Bullock and R. S. Somerville, “Observational gamma-ray cosmology,” *AIP Conf. Proc.* **745**, 23 (2005) astro-ph/0502177.
- [34] K. Shinzaki [AGASA Collaboration], “AGASA results,” *Nucl. Phys. Proc. Suppl.* **151**, 3 (2006); see also <http://www.akeno.icrr.u-tokyo.ac.jp/AGASA/>.
- [35] R. U. Abbasi *et al.* [High Resolution Fly’s Eye Collaboration], “Measurement of the flux of ultrahigh energy cosmic rays from monocular observations by the High Resolution Fly’s Eye experiment,” *Phys. Rev. Lett.* **92**, 151101 (2004) [arXiv:astro-ph/0208243].
- [36] A. W. Strong, I. V. Moskalenko and O. Reimer, “A new estimate of the extragalactic gamma-ray background from EGRET data,” arXiv:astro-ph/0306345.
- [37] D. Semikoz, G. Sigl, and O. Kalashev, in preparation.
- [38] G. Sigl, F. Miniati and T. A. Ensslin, “Ultra-high energy cosmic ray probes of large scale structure and magnetic fields,” *Phys. Rev. D* **70**, 043007 (2004) [arXiv:astro-ph/0401084]; G. Sigl, F. Miniati and T. Ensslin, “Cosmic magnetic fields and their influence on ultra-high energy cosmic ray propagation,” *Nucl. Phys. Proc. Suppl.* **136**, 224 (2004) [arXiv:astro-ph/0409098].
- [39] D. Ryu, H. Kang, and P. L. Biermann, *Astron. Astrophys.* **335** (1998) 19.
- [40] F. Miniati, “Inter-galactic Shock Acceleration and the Cosmic Gamma-ray Background,” *Mon. Not. Roy. Astron. Soc.* **337**, 199 (2002) [arXiv:astro-ph/0203014].
- [41] K. Dolag, D. Grasso, V. Springel and I. Tkachev, “Mapping deflections of Ultra-High Energy Cosmic Rays in Constrained Simulations of Extragalactic Magnetic Fields,” *JETP Lett.* **79**, 583 (2004) [Pisma Zh. Eksp. Teor. Fiz. **79**, 719 (2004)] [arXiv:astro-ph/0310902]; K. Dolag, D. Grasso, V. Springel and I. Tkachev, “Constrained simulations of the magnetic field in the local universe and the propagation of UHECRs,” *JCAP* **0501**, 009 (2005) [arXiv:astro-ph/0410419].
- [42] V. Berezhinsky and A. Z. Gazizov, “Diffusion of Cosmic Rays in the Expanding Universe. II. Energy Spectra of Ultra-High Energy Cosmic Rays,” arXiv:astro-ph/0702102.
- [43] P. Blasi, S. Bures and A. V. Olinto, “Cosmological Magnetic Fields Limits in an Inhomogeneous Universe,” *Astrophys. J.* **514**, L79 (1999) [arXiv:astro-ph/9812487].
- [44] S. j. Lee, A. Olinto and G. Sigl, “Extragalactic Magnetic Field And The Highest Energy Cosmic Rays,” *Astrophys. J.* **455**, L21 (1995) [arXiv:astro-ph/9508088].
- [45] M. Kachelriess and D. V. Semikoz, “Reconciling the ultra-high energy cosmic ray spectrum with Fermi shock acceleration,” *Phys. Lett. B* **634**, 143 (2006) [arXiv:astro-ph/0510188].
- [46] D. De Marco, T. Stanev and F. W. Stecker, “Cosmogenic neutrinos from cosmic ray interactions with extragalactic infrared photons,” *Phys. Rev. D* **73**, 043003 (2006) [arXiv:astro-ph/0512479].
- [47] D. De Marco, P. Blasi, P. Hansen and T. Stanev, “High energy neutrinos from cosmic ray interactions in clusters of galaxies,” *Phys. Rev. D* **73**, 043004 (2006) [arXiv:astro-ph/0511535].
- [48] L. A. Anchordoqui, J. F. Beacom, H. Goldberg, S. Palomares-Ruiz and T. J. Weiler, “TeV gamma-rays from photo-disintegration / de-excitation of cosmic-ray nuclei,” arXiv:astro-ph/0611580.
- [49] D. Hooper, A. Taylor and S. Sarkar, “The impact of heavy nuclei on the cosmogenic neutrino flux,” *Astropart. Phys.* **23**, 11 (2005) [arXiv:astro-ph/0407618].
- [50] L. A. Anchordoqui, D. Hooper, S. Sarkar and A. M. Taylor, “High-energy neutrinos from astrophysical accelerators of cosmic ray nuclei,” arXiv:astro-ph/0703001.
- [51] M. Ave, N. Busca, A. V. Olinto, A. A. Watson and T. Yamamoto, “Cosmogenic neutrinos from ultra-high energy nuclei,” *Astropart. Phys.* **23**, 19 (2005) [arXiv:astro-ph/0409316].
- [52] E. Armengaud, G. Sigl and F. Miniati, “Secondary gamma rays from ultrahigh energy cosmic rays produced in magnetized environments,” *Phys. Rev. D* **73**, 083008 (2006).